

Computational study on capturing CO₂ and SO₂ gases using imidazolium based ionic liquids

M. G. Awoke

Department of chemistry, College of Natural and Computational sciences, Mekdela Amba University, P.O.box:32, Tulu Awulia, Ethiopia

ARTICLE INFO

Received: 14 December 2023

Revised: 17 April 2024

Accepted: 06 May 2024

eISSN 2224-7157/© 2023 The Author(s).
Published by Bangladesh Council of
Scientific and Industrial Research
(BCSIR).

This is an open access article under the
terms of the Creative Commons Non
Commercial License (CC BY-NC)
(<https://creativecommons.org/licenses/by-nc/4.0/>)

DOI: <https://doi.org/10.3329/bjsir.v59i2.70215>

Abstract

The objective of this study was to capture CO₂ and SO₂ gases using imidazolium based ionic liquids, 1-butyl 3-methyl-imidazolium bis(trifluoromethylsulfonyl)imide and 1-ethyl 3-methyl-imidazolium acetate. In this work, the density functional theory (DFT) method of hybrid correlation functional with B3LYP/6-31++G (d, p) basis set was used to analyze the mechanism of interaction between gases and ionic liquids. It has been found that 1-butyl 3-methyl-imidazolium bis(trifluoromethylsulfonyl)imide sulfur dioxide ([C₄mim][Tf₂N]-SO₂) has greater binding energy than 1-butyl 3-methyl-imidazolium bis(trifluoromethylsulfonyl)imide carbon dioxide ([C₄mim][Tf₂N]-CO₂). Therefore, the ionic liquid, [C₄mim][Tf₂N] seems to be the most suitable option for SO₂ gas capture. Similarly, the ionic liquid, 1-ethyl 3-methyl-imidazolium acetate ([C₂mim][Ac]) has higher efficiency to capture SO₂ and has higher affinity for this gas relative to CO₂. The types of absorption observed in [C₄mim][Tf₂N]-SO₂ interaction was chemisorption while, [C₄mim][Tf₂N]-CO₂ interaction was physisorption. To sum up, [C₄mim][Tf₂N] and [C₂mim][Ac] seem to be the most suitable option to capture SO₂ gas relative to CO₂.

Keywords: CO₂ and SO₂ gas capture; Absorption; DFT; Ionic liquids; MO analysis

Introduction

Now a days, environmental pollution is a global concern. Air pollution is attracting increasing attention throughout the world. There are a lot of air pollutants released to the environment through the combustion of fossil-based fuels. SO₂ and CO₂ are the main air pollutants causing serious harm to the environment as well as human health (Smith *et al.* 2011). In addition to the risks for environment on a local scale, the mankind now faces with danger of global warming caused by greenhouse gas emissions (mainly carbon dioxide). In order to solve such greenhouse gas emission and danger of global warming, computational chemistry, which is defined as branch of chemistry that uses computer simulation to assist in solving chemical problems plays a vital role (Profeta and Kirk, 1995). It uses methods of theoretical chemistry, incorporated into efficient computer programs, to calculate the structures and properties of molecules and solids. It is the application of chemical, mathematical and computing skills to the solution of interesting chemical

problems. It uses computers to generate information such as properties of molecules or simulated experimental results (Metz *et al.* 2005).

Since computational chemistry has become easier to use, professional computational chemists have shifted their attention towards more difficult modeling problems like capturing of acid gases in liquids or adsorbents (Heede, 2014). One of the major greenhouse gases responsible for climate change is CO₂. Although CO₂ is the most relevant gas considering greenhouse effects, (Du *et al.* 2016) combustion of fossil fuels also results in the release of other toxic gases with severe environmental impact. SO₂ is another harmful gas that is released into the atmosphere and due to its acidic nature, it causes severe problems to the environment including acid rain (Raynal *et al.* 2011) and controlling acidic gas emissions is frequently considered as a global issue.

*Corresponding author's e-mail: mekumekdela21@gmail.com

In order to prevent irreversible climate change, it is crucial to reduce the CO₂ emissions and one of the options to achieve this is by the carbon capture and storage (CCS) route (Lei *et al.* 2014).

The most common capturing technologies for gas capture are based on absorption with aqueous amine solutions, which are also considered as reference methods in comparison with other alternatives which is available method for absorption of acid gases like CO₂ in soft drink industries still now (Ramdin *et al.* 2012, Luo *et al.* 2016). But, amine-based procedures have drawbacks such as amine degradation, equipment corrosion, large energy consumption for solvent regeneration and high operational costs which show the need for new technologies such as those based on ionic liquids (ILs). Nowadays, ILs are under intensive investigation due to their unique properties, such as almost negligible vapor pressure which prevents solvent losses, wide range of liquidus temperature, high thermal and chemical stability, tunable structures, and low melting point, non-flammable, low toxicity, good recyclability. These can make them a safer and more environmentally-friendly option and good solubility for many organic and inorganic materials (Cao *et al.* 2016, Schatz and Ratner, 1993). ILs are defined as liquid salts typically organic which solely consist of cations and anions, and have meager melting points (liquids below 100°C) and a very low (negligible) vapor pressure (Yim J-H *et al.* 2020). Due to their unique qualities as liquids, they have lately caught the interest of the scientific research community, as they are perfect substitutes for volatile organic solvents, which are a significant source of waste in the chemical synthesis industry (Carvalho PJ, *et al.* 2009). Ions are poorly coordinated, which result in these solvents being liquid below 100°C, or even at room temperature. Computational methodologies have been used extensively in recent times to complement experimental studies in the IL area with a great deal of success. When using computational techniques, there are three major conceptual approaches to treating a molecular system; the first is the use of electronic structure methods, which try to capture the most detailed view of a molecular system, short of solving the Schrödinger equation.

Ab initio and semi-empirical calculations are highly accurate and reliable, as they are derived directly from quantum-mechanical principles; the energy is calculated from a wave function obtained using approximations of varying quality. As a result of this, there is generally a high computational cost associated with these methods and the simulations are restricted to smaller systems. The DFT approach allows accurate quantification of the strength of IL–acidic gas interactions; intermolecular forces and molecular and physicochemical changes upon acidic gas capture (Becke, 1988).

The computational requirements for DFT calculations limit the number of molecules, yet the DFT method is still capable of providing a detailed picture of short-range interactions of IL–acidic gas systems. Wang *et al.* 2019 used a room temperature technique to remove sour gas from syngas using IL as a physical solvent. It was highlighted that ILs, such as [C₄mim][Tf₂N] could be used effectively for the removal of CO₂ by 95.3%. Imidazolium – based ionic liquids with selected anions showed large affinities both for CO₂ and SO₂ (P. Sharma *et al.* 2012).

DFT method is selected because of its low computational cost, good accuracy for structures and thermochemistry, the density is conceptually simpler than wave-function and uses approximation so that it saves time. The aim of this study was to capture some selected gases in 1-butyl-3-methyl imidazolium bis (trifluoromethylsulfonyl) imide and 1-ethyl 3-methyl-imidazolium acetate ILs. The cations and anions with respective to their atoms color code: grey- carbon, red-oxygen, yellow-sulfur, white-hydrogen, blue-nitrogen and sky-blue-fluorine of the ILs under study are shown in Figure 1.

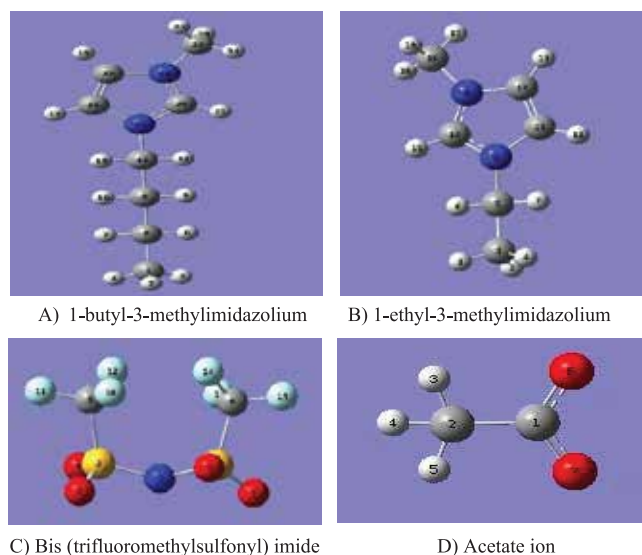


Fig. 1. The structures of cations and anions used in this study

Materials and methods

The IL and CO₂ and SO₂ gases were optimized in the gas phase using Gaussian 09 Software (Revision D.01) package (Santiago *et al.* 2011). The DFT method with Becke's Three Parameter Lee Yang & Parr correlation functional (B3LYP) and /6-31++G (d, p) basis set was used for the quantum chemical calculations (Gurau *et al.* 2011). The gas capture at the molecular level could be related with the strength of the

interactions between the ions and the gas molecules. The interaction strength was mainly analyzed *based* on binding energies (BE). The higher BE is adequate for high gas capture efficiency. Binding energy (ΔE) is defined as the energy difference between the energy sum of different complex and the sum of the energy of each component. A positive binding energy corresponds to favorable binding of the molecules (gases) to the ILs. The binding energy due to the interaction between the IL and the gas molecule is estimated as:

$$BE = E_{IL} - (E_{cat} + E_{ani} + E_{gas}) \dots \dots \dots (3.1)$$

Where E_{IL} , E_{cat} and E_{ani} stand for the energies of ILs pairs (anion plus cation complex), cations and anions, respectively.

For $ILCO_2$ and $ILSO_2$ complexes, the binding energies were calculated as:

$$\Delta E_{IL-CO_2} = E_{IL-CO_2} - (E_{cat} + E_{ani} + E_{CO_2}) \dots \dots \dots (3.2)$$

$$\Delta E_{IL-SO_2} = E_{IL-SO_2} - (E_{cat} + E_{ani} + E_{SO_2}) \dots \dots \dots (3.3)$$

The absorption energy (E_{abs}) is also estimated using the output values of gases and ILs as:

$$E_{abs} = E(\text{gas}-[C_4\text{mim}][Tf_2N]) - E([C_4\text{mim}][Tf_2N]) - (E_{gas}) \dots \dots \dots (3.4)$$

Where $E(\text{gas}-[C_4\text{mim}][Tf_2N])$, $E([C_4\text{mim}][Tf_2N])$ and E_{gas} are the energies of the gas- $[C_4\text{mim}][Tf_2N]$, $[C_4\text{mim}][Tf_2N]$, and the isolated gas, respectively.

Similarly, for the $C_2\text{mim}-Ac$, the absorption energy, E_{abs}

$$E_{abs} = E(\text{gas}-[C_2\text{mim}][Ac]) - E([C_2\text{mim}][Ac]) - (E_{gas}) \dots \dots \dots (3.5)$$

Where $E(\text{gas}-[C_2\text{mim}][Ac])$, $E([C_2\text{mim}][Ac])$ and E_{gas} are the energies of the gas- $[C_2\text{mim}][Ac]$, $[C_2\text{mim}][Ac]$, and the isolated gas, respectively.

At the molecular level, intermolecular interactions (cation-anion and ion-gas) are the key parameters related to gas capture using ILs (García *et al.* 2017).

Results and discussion

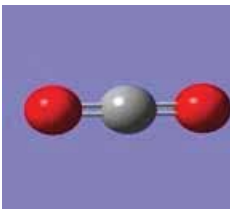
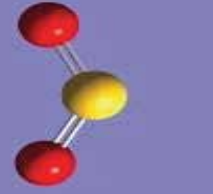
Optimized geometries of gases, ionic liquids and ionic liquid-gas interactions

Minimum energy (Optimized) structures of gases

In this work, an investigation of various intermolecular interactions between the gases and the ILs can be undertaken to understand CO_2 and SO_2 uptake in the two ILs namely $[C_4\text{mim}][Tf_2N]$ and $[C_2\text{mim}][Ac]$. The gases are fully optimized at B3LYP/6-31++G (d, p) using Gaussian 09 software. The analysis of the results was done in a gradual way, starting from the interaction of isolated ions with gas molecules, then evolving to the properties of ion pairs with the gases and finally studying the behavior of large clusters interacting with CO_2 and SO_2 molecules. The optimized geometries of gases along with their total energies and gradients of four gases used in this study are shown in Table I.

The findings in Table I illustrates that the amount of total energy needed for the optimization of gases were tabulated in decreasing order from CO_2 to SO_2 gas and the maximum and minimum total energies for the optimization of these gases were -188.5903926 and -548.599 a.u, respectively. It implies that CO had more unstable structures than the rest gases. Reversely, SO_2 has smaller amount of root-mean-square (RMS) gradient norm (0.0027998) among all the four gases.

Table I. Optimized structure with total energy and RMS Gradient Norm of gases (in a.u)

Gases	CO_2	SO_2
Optimized structure		
Total energy	-188.5903926	-548.599358
RMS Gradient Norm	0.06563623	0.00279980
Dipole Moment (D)	0.0000	1.9984

The dipole moment for CO₂ obtained as a result of the optimization geometry of CO₂ is zero since two oxygen atoms attract electrons towards itself from carbon since it has more electronegativity than carbon with the same electro negativity, and finally they becomes cancelled.

Minimum energy structures of cations and anions

ILs were also fully optimized at B3LYP/6-31++G (d, p) using Gaussian 09 software. During the optimization of cations and anions of ILs, the total energy and RMS gradient

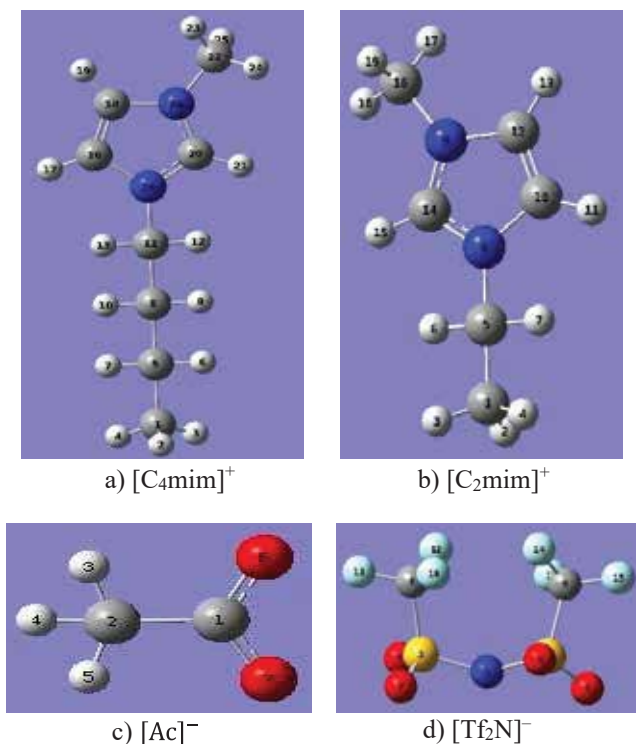


Fig. 2. Optimized geometries of cations and anions

norm versus optimization step number plots of a lot of possible structures are obtained. But the structure with the minimum energy is selected for analysis. The atoms with their color code (grey-carbon, red-oxygen, yellow-sulfur, white-hydrogen, blue-nitrogen and sky-blue-fluorine) are shown as in Figure 2. The results in Table II were obtained by optimizing the isolated ions of [C₄mim]⁺ and [C₂mim]⁺ at B3LYP/6-31++G (d, p) level. The bond length of C-N distance in the imidazolium ring of [C₄mim]⁺ is shorter than bond length of C-N bond in the imidazolium ring of [C₂mim]⁺. The shorter the distance the stronger the interactions (Handy *et al.* 2014). Therefore, the interaction among the atoms of [C₄mim]⁺ is stronger than that of the [C₂mim]⁺. The dihedral angle of some atoms in [C₄mim]⁺ shows less linearity relative to the dihedral angle of some atoms in

[C₂mim]⁺ because the dihedral angle of atoms in [C₂mim]⁺ have exactly 180° which is exactly linear. The bond length of C-N bond for both [C₄mim]⁺ and [C₂mim]⁺ was in the range of 1.338 Å and 1.470 Å. From the bond angle results, it can be observed that most of the carbon and nitrogen bond angles of the [C₄mim]⁺ are smaller than the bond angles of carbon and nitrogen in [C₂mim]⁺ and this also shows that the bonds are shortened due to the strong interactions on [C₄mim]⁺ than [C₂mim]⁺.

Minimum energy structures of ionic liquid cation-anion interactions

The cation-anion interactions of the ILs in this study were fully optimized at B3LYP/6-31++G (d, p). To obtain the most stable structure of [C₂mim][Ac], the acetate ion was located at different average position of 1-ethyl-3-methylimidazolium around the imidazolium ring and one of the oxygen atom of acetate ion was found near to the imidazolium ring of H-18 attached to C-17 and another H-25 attached to C-23 of [C₂mim][Ac] as shown in Figure 3 and similarly, the most stable structure of [C₄mim][Tf₂N] was obtained as displayed in Figure 4. As presented in Table III, the C-N

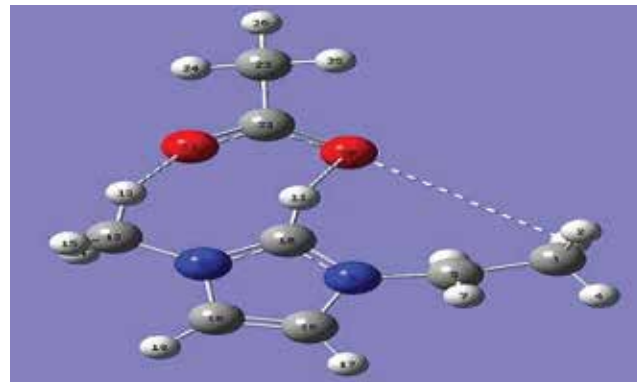


Fig. 3. The most stable geometry of [C₂mim][Ac]

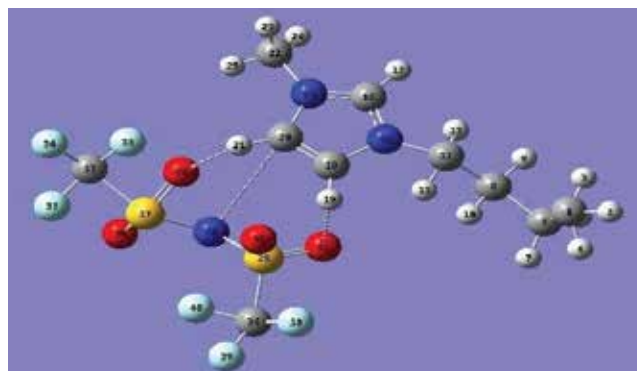


Fig. 4. The most stable structure of [C₄mim][Tf₂N]

Table II. Bond lengths, angles and dihedral angles of some of the most stable [C₄mim]⁺ and [C₂mim]⁺ cations calculated at the B3LYP/6-31++G (d,p) level

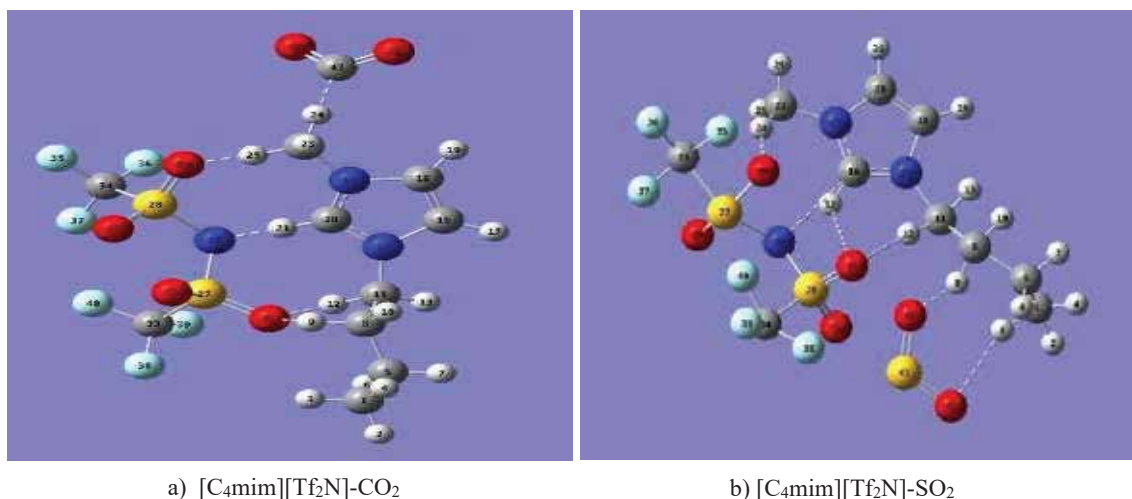
Atoms	[C ₄ mim] ⁺ (Å)	Atoms	[C ₂ mim] ⁺ (Å)
N14–C20	1.383	C14–N9	1.467
N15–C22	1.4700	C12–C14	1.345
C16–N14	1.338	N9–C16	1.470
N14–C11	1.470	C10–N8	1.346
C1–C5	1.540	N8–C12	1.467
Atoms	[C ₄ mim] ⁺ (°)	Atoms	[C ₂ mim] ⁺ (°)
∠N15–C18–C20	37.547	∠C14–C12–N9	38.412
∠N14–C16–C18	32.546	∠C10–N8–C12	33.989
∠C16–C14–N15	35.323	∠C12–C14–N8	106.858
∠C20–C18–N15	106.859	∠N9–C14–C16	27.145
∠N14–C16–C20	71.807	∠N8–C5–C10	25.823
Atoms	[C ₄ mim] ⁺ (D, deg)	Atoms	[C ₂ mim] ⁺ (D, deg)
DN14–N15–C20–C22	-179.976	DN9–C10–N8–C5	180.00
DN15–C16–N14–C22	-179.997	DC14–C12–N8–C5	180.00
DC11–N14–C16–C22	179.993	DC16–N9–C10–N8	-180.00

Å - bond lengths, (°) - angles and D, deg - dihedral

Table III. Bond lengths, angles and dihedral angles of some of the most stable [C₄mim][Tf₂N] and [C₂mim][Ac] ionic liquids calculated at the B3LYP/6-31++G (d,p) level

Atoms	[C ₄ mim][Tf ₂ N] (Å)	Atoms	[C ₂ mim][Ac] (Å)
C29–N26	3.547	H13–O21	2.102
H19–O32	1.589	H11–O20	2.226
O29–H21	4.207	C10–N9	1.582
Atoms	[C ₄ mim][Tf ₂ N] (°)	Atoms	[C ₂ mim][Ac] (°)
∠S28–N26–C34	109.471	∠C22–O22–O20	125.637
∠S27–O29–C33	82.557	∠N9–C18–C10	111.060
∠C33–F35–F36	81.784	∠C18–C16–N8	106.250
∠N14–C11–C16	125.768	∠C10–N9–N8	99.366
Atoms	[C ₄ mim][Tf ₂ N] (D, deg)	Atoms	[C ₂ mim][Ac] (D, deg)
D N26–S27–C33–C36	149.832	D C1–C2–O22–C8	151.274
D N26–S27–S28–C34	90.00	D C8–C12–N9–C17	-90.000
D N26–S28–O32–C34	-120.00	D C23–N8–C21–C19	-180.00
D C8–C11–N14–C16	-91.546	D C21–C19–N9–C12	180.00

Å - bond lengths, (°) - angles and D, deg - dihedral angles

a) [C₄mim][Tf₂N]-CO₂b) [C₄mim][Tf₂N]-SO₂**Fig. 5.** The [C₄mim][Tf₂N]-gas optimized minimum energy structures**Table IV.** Bond lengths, angles and dihedral angles of the most stable [C₄mim][Tf₂N]-CO₂ and [C₄mim][Tf₂N]-SO₂ ionic liquids calculated at the B3LYP/6-31++G (d,p) level

Atoms	[C ₄ mim][Tf ₂ N]-CO ₂ (Å)	Atoms	Atoms	[C ₄ mim][Tf ₂ N]-SO ₂ (Å)
O29-H25	1.342	O31-H12	O29-H25	2.676
H24-C43	1.151	O29-H24	H24-C43	1.873
O31-H9	1.367	O42-H9	O31-H9	1.663
N26-H21	1.939	N26-C16	N26-H21	2.668

Atoms	[C ₄ mim][Tf ₂ N]-CO ₂ (°)	Atoms	[C ₄ mim][Tf ₂ N]-SO ₂ (°)
⟨C43-O41-O42	127.999	⟨S28-C34-N26	109.471
⟨S27-O29-N26	89.577	⟨S27-C33-O29	42.598
⟨N26-S27-S28	125.963	⟨S41-O42-O43	30.00
⟨C16-N15-N14	109.150	⟨C16-N14-N15	35.323
⟨C20-N15-C18	35.200	⟨N14-C16-C18	37.547

Atoms	[C ₄ mim][Tf ₂ N]-CO ₂ (D, deg)	Atoms	[C ₄ mim][Tf ₂ N]-SO ₂ (D, deg)
D C33-S27-N26-S28	-159.366	D N26-S27-S28-O31	-90.00
D S27-N26-S28-O32	154.372	D N26-S27-S28-O29	150.00
D O43-C41-O42-C22	172.693	D C8-C11-N14-C16	-91.546
D C22-C16-N15-N14	-156.468	D C11-N14-N15-C20	-180.00

Å - bond lengths, (°) - angles and D, deg - dihedral angles

bond length in $[C_4mim][Tf_2N]$ was shorter than C-N bond length of $[C_2mim][Ac]$ which shows that the cation-anion interaction in the $[C_4mim][Tf_2N]$ was stronger than that of $[C_2mim][Ac]$ from the idea that the shorter the distance was the stronger the interactions (Handy *et al.* 2014).

The cation-anion distance H19-O32 (1.589Å) of $[C_4mim][Tf_2N]$ was shorter than the cation-anion distance H11-O20 (2.226Å) of $[C_2mim][Ac]$. Therefore, there was stronger anion-cation interactions in the $[C_4mim][Tf_2N]$ than $[C_2mim][Ac]$. With regard to the bond angles, sulphur has 109.47° in the $[C_4mim][Tf_2N]$ ion pair shows tetrahedral types of geometry and the dihedral angle results illustrates that the presence of both negative and positive angles corresponds to clockwise and anti-clock wise rotations (Richardson, 1981). The dihedral angles of $[C_2mim][Ac]$ shows better linearity than that of $[C_4mim][Tf_2N]$.

Minimum energy structures of $[C_4mim][Tf_2N]$ -gas interactions

The optimized structure of gases, cations and anions were optimized together at B3LYP/6-31++G (d, p). The gases such as CO_2 and SO_2 were placed at average position around the 1-butyl-3-methyl imidazolium bis (trifluoro sulfonyl methyl) imide ILs and the optimization were done. Upon optimization, the optimized result provides a lot of possible structures with total energy and root mean square gradient norm versus optimization step number. But the global minimum energy structure was taken in to account for further analysis. Figure 5 shows the most stable structures for $[C_4mim][Tf_2N]$ -gas.

The $[C_4mim][Tf_2N]-CO_2$ molecule is shown in Figure 5(a) in which CO_2 gas is located around the optimized structure of $[C_4mim][Tf_2N]$ in the left side of Tf_2N ion, in the right side of $[C_4mim]^+$ below the average distance of $[C_4mim][Tf_2N]$ and above the average distance of $[C_4mim][Tf_2N]$ and then after 120 optimization steps, C-43 of the CO_2 gas near to H-24 attached with C-22 of the imidazolium ring is obtained as the minimum energy structure of the IL-gas interaction. Figure 5 (b) shows the optimized stable structure of $[C_4mim][Tf_2N]-SO_2$ which is placing the SO_2 gas around the average position of $[C_4mim][Tf_2N]$. In this case, one of the oxygen atoms of SO_2 is near the H-9 attached to C-8 which is far away from the imidazolium ring. The atoms with their color code (carbon-gray, oxygen-red, nitrogen-blue, hydrogen-white, Sulphur-yellow, fluorine-sky blue) were shown as in Figure 5.

The optimized geometry parameters such as the bond lengths, angles, and dihedral angles for $[C_4mim][Tf_2N]$ with SO_2 and CO_2 calculated at the B3LYP/6-31++G (d,p) level of

theory are shown above. The results in Table IV show that the O-H bond length in the ion-pair $[C_4mim][Tf_2N]-SO_2$ was shorter than the ion pair $[C_4mim][Tf_2N]-CO_2$ which implies that the IL-gas interaction was stronger in the ion pair $[C_4mim][Tf_2N]-SO_2$ than the ion pair $[C_4mim][Tf_2N]-CO_2$. The cation-anion distance O29-H25(1.342Å) of $[C_4mim][Tf_2N]-CO_2$ was shorter than the anion-cation distance O31-H12 (2.676Å) of $[C_4mim][Tf_2N]-SO_2$ in the results given in Table IV. This shows that the interaction among the molecules was stronger in the first ion pair than that of the second ion pair. The cation-gas bond length for H24-C43 (1.151Å) in $[C_4mim][Tf_2N]-CO_2$ is shorter than cation-anion bond length for O31-H9 (1.3671Å) and the cation-gas bond length for O42-H9 (1.663Å) in $[C_4mim][Tf_2N]-SO_2$ was shorter than cation-anion bond

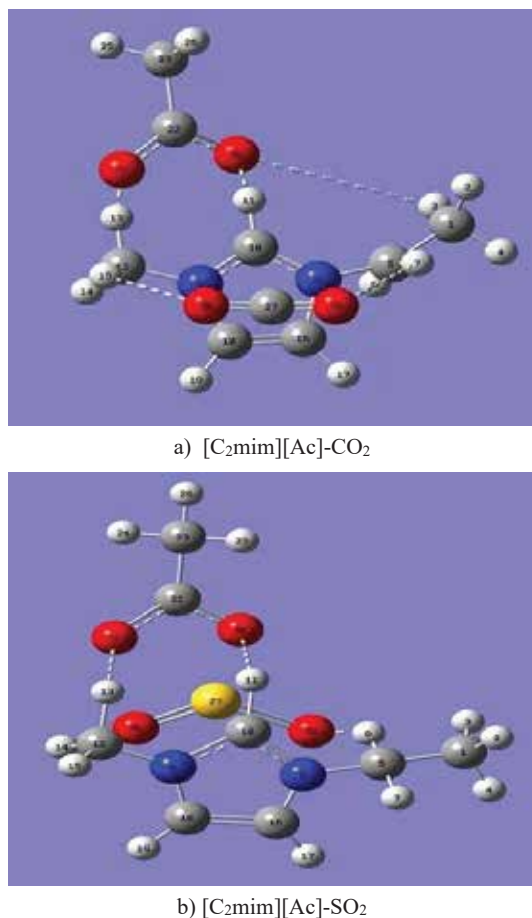


Fig. 6. The $[C_2mim][Ac]$ -gas optimized minimum energy structures

length for O29-H12 (1.873Å). Therefore, the cation-gas interaction was stronger than the cation anion interaction in both ion pairs [20]. The bond angle provided for sulphur (S28) shows tetrahedral structure in $[C_4mim][Tf_2N]-SO_2$ and

the angle of C16 in [C₄mim][Tf₂N]-CO₂ also shows tetrahedral geometry. The dihedral angle result reflects the presence of clock wise and anti-clock wise rotations in both ion pairs.

Minimum energy structures of [C₂mim][Ac]-gas interactions

The optimized structure of gases, cations and anions were optimized together at B3LYP/6-31++G (d, p). The gases such as CO₂, SO₂ were placed at average position around the 1-ethyl-3-methyl imidazolium acetate ILs in order to guess the most stable (lowest energy) structure and the optimizations are done. Upon optimization, the optimized result provides a lot of possible structures with energy and RMS gradient norm versus optimization step number. But the global minimum energy structure for [C₂mim][Ac]-gas was taken in to account for further analysis.

The optimized minimum energy structure of [C₂mim][Ac]-CO₂ was given in Figure 6 (a). This structure is obtained as a result of locating the CO₂ gas around the average position of the optimized structure of [C₂mim][ac], the CO₂ was near to the imidazolium ring and far from the acetate ion. The most stable structure of [C₂mim][Ac]-SO₂ is given in Figure 6 (b) which was obtained as a result of locating the SO₂ gas around the average position of the optimized structure of [C₂mim][Ac] and the SO₂ is found near to the imidazolium ring while a bit far from the acetate

ion. The bond lengths, angles and dihedral angles of the most stable structures of [C₂mim][Ac]-SO₂ and [C₂mim][Ac]-CO₂ calculated at the B3LYP/6-31++G (d,p) level are shown in Table V.

The results in Table V show that the bond length of C-N (1.270Å) in [C₂mim][Ac]-SO₂ was shorter than the bond length of C-N (1.342Å) in [C₂mim][Ac]-CO₂. So that the interactions among the molecules in [C₂mim][Ac]-SO₂ was stronger than those of [C₂mim][Ac]-CO₂. The cation-gas distance of S27-C10 (1.354Å) in [C₂mim][Ac]-SO₂ was shorter than the cation-gas distance of C18-O28 (2.839Å) in [C₂mim][Ac]-CO₂ implies that the cation-gas interaction is stronger in [C₂mim][Ac]-SO₂ than in [C₂mim][Ac]-CO₂. Cation-anion interaction was stronger than cation-gas interactions in [C₂mim][Ac]-CO₂ whereas, cation-gas interaction of [C₂mim][Ac]-SO₂ dominates the cation-anion interactions.

DFT analysis of binding energy and absorption energy for [C₄mim][Tf₂N]-gas and [C₂mim][Ac]-gas interactions

Gas capture at the molecular level could be related with the strength of the interactions between the ions and the gas molecule. In this work, the interaction strength has been mainly analyzed based on BEs (García *et al.* 2015). Then after the gases, IL and IL-gas interaction optimizations, the

Table V. Bond lengths, angles and dihedral angles of the most stable [C₂mim][Ac]- SO₂ and [C₂mim][Ac]-CO₂ ionic liquids calculated at the B3LYP/6-31++G (d,p) level

Atoms	[C ₂ mim][Ac]-SO ₂ (Å)	Atoms	[C ₂ mim][Ac]-CO ₂ (Å)
N9-C10	1.332	N9-C10	1.342
N8-C16	1.270	N9-C18	1.388
S27-C10	1.354	C18-O28	2.839
O28-H6	1.046	N9-O28	2.826
H13-O21	2.070	O20-H11	1.443
H13-O21	2.070	O20-H11	1.443
Atoms	[C ₂ mim][Ac]-SO ₂ (°)	Atoms	[C ₂ mim][Ac]-CO ₂ (°)
⟨C22-O20-O21	110.337	O21-H13	1.136
⟨S27-O28-O29	127.992	⟨C27-O28-O29	178.194
⟨N8-C10-C16	116.429	⟨N9-C10-N8	108.573
Atoms	[C ₂ mim][Ac]-SO ₂ (D, deg)	Atoms	[C ₂ mim][Ac]-CO ₂ (D, deg)
D O20-C10-C22-N8	169.032	⟨N9-C18-C16	107.172
D N9-C16-C18-C12	179.828	D O28-C27-O29-C5	-110.729
D C10-C5-N8-N9	170.735	D N8-C10-O20-C22	-164.617

Å - bond lengths, (°) - angles and D, deg - dihedral angles

Table VI. [C₄mim][Tf₂N] -gas interaction binding energy

IL-gas interactions	$E_{\text{IL-gas}}$ (eV)	Cations		Gas	E_{gas} (eV)	BE (kJ/mol)
		E (C ₄ mim)	E (Tf ₂ N)			
[C ₄ mim][Tf ₂ N]-CO ₂	-66371.541	-11519.95	-49723.294	CO ₂	-5131.019	262.63
[C ₄ mim][Tf ₂ N]-SO ₂	-76168.724	-11519.95	-49723.294	SO ₂	-14928.257	267.94

binding energy of the interacting molecule is calculated using equation (3.1) and the results are tabulated in Table VI which were obtained by calculating the BE of IL-gas interaction according to equation (3.1). The results illustrate that [C₄mim][Tf₂N]-SO₂ has greater binding energy compared to [C₄mim][Tf₂N]-CO₂ which is approximately similar with the BE obtained by Gregorio Garcí'a *et al.* 2015 (339.0 kJ/mol). G. B. Damas *et al.* 2014 revealed that the values of BE in literature (360kJ/mol), the BE of [C₄mim][Tf₂N]-SO₂ is lower (267.94 kJ/mol) than the findings in this research but higher than other literature findings (31.70-60.30kJ/mol). Therefore, the [C₄mim][Tf₂N] seems to be the most suitable option for SO₂ gas capture. Since the higher BEs will be adequate for high gas capture efficiency (García *et al.* 2015). The [C₄mim][Tf₂N] has high SO₂ gas capture efficiency relative to the other two gases. The types of absorption can be differentiated based on the results of binding energies of IL-gas interactions. Binding energies of IL...SO₂ systems have been used as a measurement of the interaction strength between selected ILs and SO₂ molecule (Yang *et al.* 2013). Chemical absorption is characterized by the formation of a solute-solvent adduct due to strong localized interaction (Gurau *et al.* 2011). The higher BEs correspond to the stronger the interactions between the

VII. Among the two ion-pairs, [C₄mim][Tf₂N]-SO₂ has greater absorption energy which indicates that there was a strong interaction with in [C₄mim][Tf₂N]. The higher absorption energy shows that the chemisorption of SO₂ on to [C₄mim][Tf₂N] and the lower absorption energy shows the physisorption of CO₂ on to the IL (García *et al.* 2017). According to Li, L *et al.* 2013, the BE and the absorption enthalpy of anion-CO₂ complexes, implying much stronger interactions of complexes governing larger gas solubility. The BE and absorption of the interacting molecule was calculated using equation (3.1) and the results was tabulated in Table VIII.

The result in Table VIII was obtained by calculating the binding energy of IL-gas interactions using equation (3.1). The results in this table shows that the correlation between BE and the efficiency of ILs to capture the gases that means the higher the BE would be adequate to provide high gas absorption affinities (García *et al.* 2015). The greater binding energy of [C₂mim][Ac]-SO₂ in the results above shows that [C₂mim][Ac] has higher efficiency to capture SO₂ and has higher affinity for this gas relative to CO₂. (EtNH₃)⁺-SO₂ provided the highest binding energy (578.34 kJ/mol) among all studied cations but less than that of this research findings (1,286.5 kJ/mol) based on ethyl amine cation and ethyl imidazolium cation respec-

Table VII. Absorption energy of [C₄mim][Tf₂N]-gas pairs

IL-gas	$E_{\text{IL-gas}}$ (eV)	$E_{\text{cat-ani}}$ (eV)	Gas	E_{gas} (eV)	E_{abs} (eV)
[C ₄ mim][Tf ₂ N]-CO ₂	-66371.541	-61240.713	CO ₂	-5131.019	0.191
[C ₄ mim][Tf ₂ N]-SO ₂	-76168.724	-61240.713	SO ₂	-14928.257	0.246

gases and ILs so that the types of absorption observed in [C₄mim][Tf₂N]-SO₂ interaction was chemisorption whereas the types of absorption observed in [C₄mim][Tf₂N]-CO₂ interaction was physisorption.

The absorption energy of [C₄mim][Tf₂N]-gas pairs was calculated according to Equation 3.6, as shown in Table

tively. This implies that imidazolium based ILs are better for SO₂ capture relatively (Gregorio Garcí'a *et al.* 2015). In concordance with Damas's work, the binding energy for the imidazolium family decreases upon alkyl side chain elongation. In fact, from [EMIM]⁺ to [HMIM]⁺. This agrees with the present work (from [C₂mim]⁺ to [C₄mim]⁺ given by Table VI and VIII). The absorption type observed

Table VIII. The binding energy of [C₂mim][Ac]-gas

IL-gas interactions	E_{IL-gas} (eV)	Cation	Anion	Gases	E_{gas} (eV)	BE (kJ/mol)
		E (C ₂ mim) (eV)	E (Ac) (eV)			
[C ₂ mim][Ac]-CO ₂	-20,715.184	-9,373.634	-6,217.633	CO ₂	-5131.019	685.236
[C ₂ mim][Ac]-SO ₂	-30,506.190	-9,373.634	-6,217.633	SO ₂	-14928.257	1,286.531

Table IX: Absorption energy of [C₂mim][Ac]-gas pairs

IL-gas	E_{IL-gas} (eV)	$E_{cat-ani}$ (eV)	Gas	E_{gas} (eV)	E_{abs} (eV)
[C ₂ mim][Ac]- CO ₂	-20,715.184	15,594.288	CO ₂	-5131.019	10.123
[C ₂ mim][Ac]- SO ₂	-30,506.190	15,594.288	SO ₂	-14928.257	16.355

Table X. Higher Occupied Molecular Orbital (HOMO) and Lower Unoccupied Molecular Orbital (LUMO) energies of cation-an ion and IL-gas interactions

Cation-Anion and IL-gas interactions	HOMO (a.u)	Energy LUMO Energy (a.u)	HOMO-LUMO gap (eV)	Hardness (a.u)
[C ₂ mim][Ac]	-0.3003	-0.1965	2.825	1.41
[C ₄ mim][Tf ₂ N]	-0.2538	-0.2422	0.316	0.15
[C ₂ mim][Ac]-SO ₂	-0.2747	-0.2221	1.431	0.72
[C ₂ mim][Ac]-CO ₂	-0.2273	-0.1867	1.105	0.55
[C ₄ mim][Tf ₂ N]-SO ₂	-0.3601	-0.0821	7.565	3.78
[C ₄ mim][Tf ₂ N]-CO ₂	-0.3110	-0.1349	4.792	2.40

in the [C₂mim][Ac]-SO₂ was chemical absorption. But the absorption type observed in [C₂mim][Ac]-CO₂ is physical absorption. Likewise, the absorption energy of [C₂mim][Ac]-gas pairs was calculated according to Equation 3.7, as shown in Table IX.

The results in Table IX were obtained by optimizing ILs and gases at B3LYP/6-31++G(d,p) level. The higher absorption energy in the ion pair [C₂mim][Ac]-SO₂ shows that there was a strong interaction between [C₂mim][Ac] and SO₂ whereas the lower absorption energy in the ion pair [C₂mim][Ac]-CO₂ shows that the CO₂ was easily desorbed from the ion pair CO₂-[C₂mim][Ac]. The high absorption energy indicates chemisorption of SO₂ on to [C₂mim][Ac] and the low absorption energy in the ion pair CO₂-[C₂mim][Ac] shows that weak physisorption of CO₂ on to [C₂mim][Ac] (García *et al.* 2015).

Results from molecular orbital analysis

The results obtained by the molecular orbital (MO) analysis are tabulated in Figure 7, which show the molecular orbital analysis of cations and ILs and IL-gas interactions. The [C₄mim]⁺ is shown in Figure 7 (a) in which electron density of HOMO was concentrated on the alkyl chain including the imidazolium ring. But in case of LUMO, the electron density is concentrated far from the imidazolium ring. Figure 7 (b) showed that the HOMO-LUMO diagrams of [C₂mim]⁺ in which the electron density in both HOMO and LUMO orbitals is concentrated almost all over the cations of [C₂mim]⁺. The HOMO-LUMO diagram of [C₂mim][Ac] is shown in Figure 7 (c) in which there is more electron density concentrated on the HOMO of [C₂mim][Ac] than the LUMO of this ion-pair. Therefore, there is strong cation-anion interaction in the case of the HOMO orbitals of

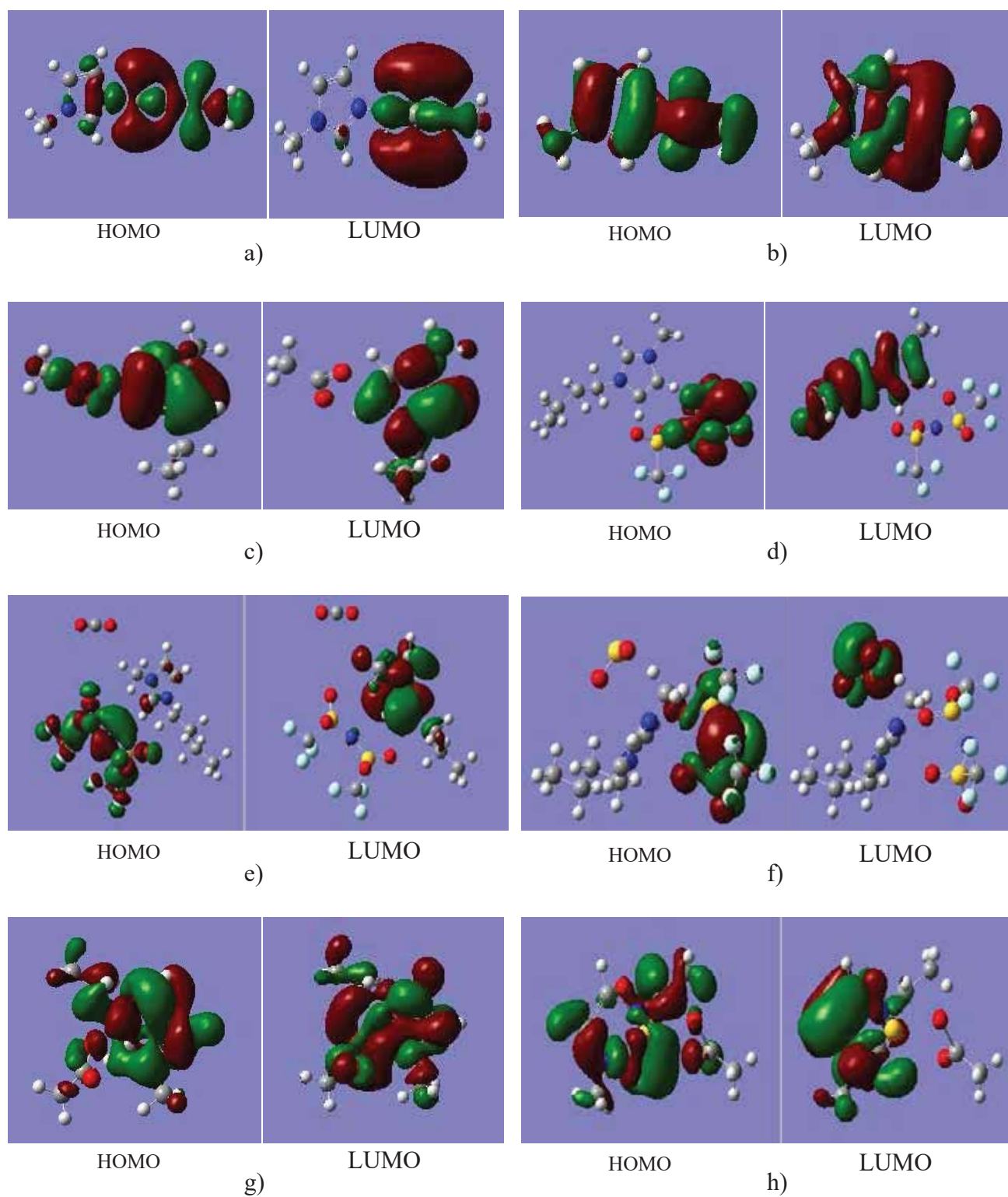


Fig. 7. HOMO-LUMO diagrams of (a) $[C_4mim]^+$ (b) $[C_2mim]^+$ (c) $[C_2mim][Ac]$ (d) $[C_4mim][Tf_2N]$ (e) $[C_4mim][Tf_2N]-CO_2$ (f) $[C_4mim][Tf_2N]-SO_2$ (g) $[C_2mim][Ac]-CO_2$ (h) $[C_2mim][Ac]-SO_2$

[C₂mim][Ac] than the LUMO due to the more overlapping of the atomic orbitals of the cations and anions. Figure 7 (d) shows the HOMO-LUMO diagram of [C₄mim][Tf₂N]. Here the electron density is concentrated on the anions of Tf₂N in HOMO and on the [C₄mim]⁺ cations in the LUMO. Therefore, there is more interaction due to the orbital overlapping of the atomic orbitals of the cations and anions in [C₂mim][Ac] than [C₄mim][Tf₂N]. [C₄mim][Tf₂N]-CO₂ is shown in Figure 7(e) in which the electron density is fully concentrated on the anions of the [C₄mim][Tf₂N] in the HOMO orbital diagram and partially concentrated on the cations of [C₄mim][Tf₂N] in the LUMO orbital diagram.

Therefore, the interaction is slightly stronger in the HOMO than the LUMO. Figure 7 (f) shows the MO diagram of [C₄mim][Tf₂N]-SO₂ in which the electron density is more concentrated on the anions and some of the cations in the HOMO orbital and in the case of LUMO, the electron density is more concentrated either of the ions but on the SO₂ gas. So that there is more interaction on the HOMO of the [C₄mim][Tf₂N]-SO₂ due to more overlapping of atomic orbitals. [C₂mim][Ac]-CO₂ is shown in Figure 7(g) such that the electron density more concentrated on the LUMO orbital diagram than that of the HOMO orbital diagram which results the stronger interaction between the ILs and gases is observed in the LUMO orbital diagrams of the [C₂mim][Ac]-CO₂ due to more overlapping of orbitals.

Compared to [C₄mim][Tf₂N]-CO₂, the electron density concentration of [C₂mim][Ac]-CO₂ was much greater than that of [C₄mim][Tf₂N]-CO₂. Figure 7 (h) showed the HOMO-LUMO diagram of [C₂mim][Ac]-SO₂. Here the electron density was more concentrated on the cations and gas and some of the anions in the HOMO orbital. In case of LUMO orbital no electron was concentrated on the anion of the ILs. So that there was more IL- gas interaction on the HOMO orbital of [C₂mim][Ac]-SO₂. The energy parameters such as HOMO and LUMO energies as well as global hardness of cation-anion and IL-gas interactions calculated at the B3LYP/6-31++G (d,p) level are summarized in Table X. The results are obtained by optimizing the ILs -gas interacted molecule at B3LYP/6-31++G (d, p) level. These results show that LUMO is always higher in energy than HOMO. The HOMO-LUMO gap is taken as subtracting HOMO from LUMO. The magnitude of the HOMO-LUMO gap has very important chemical implications, even if qualitatively evaluated. The large HOMO-LUMO energy gaps for [C₄mim][Tf₂N]-SO₂ suggests a good stability, high chemical hardness and less reactivity for the [C₄mim][Tf₂N]-SO₂ interactions (García *et al.* 2015). Indeed, the chemical hardness of the [C₄mim][Tf₂N] is the

smallest one, which indicates that this complex is more unstable than the other as presented in the table above. A large energy gap implies good thermodynamic stability of the compound, whereas a small energy gap suggests an easy electronic transition. The larger is the gap, the higher the stability, the harder the molecule (complex). Therefore, [C₄mim][Tf₂N]-SO₂ is having the largest gap, the higher stability, and the harder molecule in this result.

Conclusion

A systematic study on the relative IL-gas interaction energies of imidazolium based ILs was carried out in this work by DFT method, B3LYP/6-31++G (d,p). Based on the results obtained from DFT calculations, the following conclusions were drawn. The [C₄mim][Tf₂N]-SO₂ has the greater BE than [C₄mim][Tf₂N]-CO₂. Therefore, the [C₄mim][Tf₂N] seems to be the most suitable option for SO₂ gas capture. Since the higher BEs will be adequate for high gas capture efficiency, the IL, [C₄mim][Tf₂N] has high efficiency to capture SO₂ gas. Chemisorption is characterized by higher BEs so that the types of absorption observed in [C₄mim][Tf₂N]-SO₂ interaction was chemisorption whereas the types of absorption observed in [C₄mim][Tf₂N]-CO₂ interaction was physisorption. The ion pair [C₄mim][Tf₂N]-SO₂ has greater absorption energy which indicates that there was a strong interaction of SO₂ on [C₄mim][Tf₂N]. The higher absorption energy shows that the chemisorption of SO₂ on to [C₄mim][Tf₂N]. Physisorption was observed in the ion pairs [C₄mim][Tf₂N]-CO₂ and interaction with lower binding energies and absorption energies.

The higher absorption energy in the ion pairs [C₂mim][Ac]-SO₂ shows that there was a strong interaction between [C₂mim][Ac] and SO₂ gas. The high absorption energy indicates strong chemisorption of SO₂ on to [C₂mim][Ac] and the low absorption energy in the ion pair [C₂mim][Ac]-CO₂ showed weak physisorption of CO₂ on to [C₂mim][Ac].

Regarding the intermolecular interaction, the IL-gas interaction and the interaction among the molecules was stronger in the ion pair [C₄mim][Tf₂N]-SO₂ than the ion pair [C₄mim][Tf₂N]-CO₂. Likewise, the cation-gas interaction was stronger than the cation-anion interaction in the ion pairs [C₂mim][Ac]-SO₂ than [C₂mim][Ac]-CO₂ and the interactions among the molecules in [C₂mim][Ac]-SO₂ was also stronger than that of [C₂mim][Ac]-CO₂. Cation-anion interaction was stronger than cation-gas interactions in [C₂mim][Ac]-CO₂ whereas,

cation-gas interaction of [C₂mim][Ac]-SO₂ dominates the cation-anion interactions. The HOMO-LUMO gap for [C₄mim][Tf₂N]-SO₂ has the highest energy gap and highest chemical hardness of the rest of the IL- gas interactions and so that the most stable compound of [C₄mim][Tf₂N]-SO₂ from molecular orbital analysis was obtained.

References

- Becke AD (1988), Density-functional exchange-energy approximation with correct asymptotic behavior, *Physical review A* **38**(6): 30-98. <https://doi.org/10.1103/PhysRevA.38.3098>
- Cao B, Du J, Liu S, Zhu X, Sun X, Sun H and Fu H (2016), Carbon dioxide capture by amino-functionalized ionic liquids: DFT based theoretical analysis substantiated by FT-IR investigation, *RSC Advances* **6**(13): 10462-10470. DOI: 10.1039/C5RA23959A
- Carvalho PJ (2009), High pressure phase behavior of carbon dioxide in 1-butyl-3- methylimidazolium bis (trifluoromethylsulfonyl) imide and 1-butyl-3-methylimidazolium dicyanamide ionic liquids, *J Supercrit Fluids* **50**(2): 105-11. <https://doi.org/10.1016/j.supflu.2009.05.008>
- Du Y, Wang Y and Rochelle GT (2016), Thermal degradation of novel piperazine- based amine blends for CO₂ capture, *International Journal of Greenhouse Gas Control* **49**: 239-249. <https://doi.org/10.1016/j.ijggc.2016.03.010>
- Damas GB, Dias ABA, Costa LT, Phys J and Chem B (2014), **118**: 9046-9064.
- García Moreno GJ, Atilhan M and Aparicio Martínez S, (2015), A density functional theory insight towards the rational design of ionic liquids for SO₂ capture, *Physical Chemistry Chemical Physics* **17**(20): 13559-13574. DOI: 10.1039/C5CP00076A
- García G, Atilhan M and Aparicio S (2017), Simultaneous CO₂ and SO₂ capture by using ionic liquids: a theoretical approach, *Physical Chemistry Chemical Physics* **19**(7): 5411-5422.
- Gregorio Garcí'a, Mert Atilhan and Santiago Aparicio (2015), A density functional theory insight towards the rational design of ionic liquids for SO₂ capture. *Phys, Chem. Chem. Phys.* **(17)**: 13559. DOI: 10.1039/C5CP00076A
- Gurau G, Rodríguez H, Kelley SP, Janiczek P, Kalb RS and Rogers RD (2011), Demonstration of chemisorption of carbon dioxide in 1, 3-dialkylimidazolium acetate ionic liquids, *Angewandte Chemie International Edition* **50**(50): 12024-12026.
- Handy H, Santoso A, Widodo A, Palgunadi J, Soerawidjaja TH and Indarto A (2014), H₂S-CO₂ separation using room temperature ionic liquid [BMIM][Br]. *Separation Science and Technology* **49**(13): 2079-2084.
- Heede R (2014), Tracing anthropogenic carbon dioxide and methane emissions to fossil fuel and cement producers, 1854-2010. *Climatic Change* **122**(1-2): 229-241.
- Lei Z, Dai C and Chen B (2014), Gas solubility in ionic liquids, *Chemical reviews* **114**(2): 1289-1326.
- Li L, Zhao N, Wei W and Sun Y (2013), A review of research progress on CO₂ capture, storage, and utilization in Chinese Academy of Sciences. *Fuel*. <https://doi.org/10.1021/cr300497a>
- Luo XY, Fan X, Shi GL, Li HR and Wang CM (2016), Decreasing the viscosity in CO₂ capture by amino-functionalized ionic liquids through the formation of intramolecular hydrogen bond, *The Journal of Physical Chemistry B* **120**(10): 2807-2813. <https://doi.org/10.1021/acs.jpcc.5b10553>
- Metz B, Davidson O, De Coninck HC, Loos M and Meyer LA (2005), IPCC, 2005: IPCC special report on carbon dioxide capture and storage.
- Profeta S and Kirk J (1995), *Orthmer encyclopedia of chemical technology supplement*, John Wiley and Sons, p 315
- Ramdin M, de Loos TW and Vlugt TJ (2012), State-of-the-art of CO₂ capture with ionic liquids, *Industrial & Engineering Chemistry Research*, **51**(24): 8149-8177. <https://doi.org/10.1021/ie3003705>
- Raynal L, Bouillon PA, Gomez A and Broutin P (2011), From MEA to demixing solvents and future steps, a roadmap for lowering the cost of post-combustion carbon capture, *Chemical Engineering Journal*,

- 171**(3): 742-752. <https://doi.org/10.1016/j.ccej.2011.01.008>
- Richardson JS (1981), The anatomy and taxonomy of protein structure. In *Advances in protein chemistry*, Academic Press. **34**: 167-339. [https://doi.org/10.1016/S0065-3233\(08\)60520-3](https://doi.org/10.1016/S0065-3233(08)60520-3)
- Santiago Aparicio (2011), Study on Hydroxylammonium-Based Ionic Liquids. II. Computational Analysis of CO₂ Absorption, *J. Phys. Chem* **115**: 12487-12498. <https://doi.org/10.1021/jp206210e>
- Schatz GC and Ratner MA (1993), *Quantum mechanics in chemistry*. Courier Corporation
- Sharma P, Park SD, Baek IH, Park KT, Yoon TI and Jeong SK (2012), *Fuel Process. Technol.* **100**: 55- 62.
- Simon S Duran M and Dannenberg JJ (1970), *J. Chem. Phys.*, 1996, 105, 11024; S. F. Boys and F. Bernardi, *Mol. Phys.*, 1970, 19, 553-566.
- Smith SJ, van Aardenne J, Klimont Z, Andres RJ, Volke A and Delgado Arias S (2011), Anthropogenic sulfur dioxide emissions: 1850-2005, *Atmospheric Chemistry and Physics* **11**(3): 1101-1116.
- Sun Q, Wang M, Li Z, Du A and Searles DJ (2014), A computational study of carbon dioxide adsorption on solid boron, *Physical Chemistry Chemical Physics* **16**(25): 12695-12702.
- Wang Y (2019), A novel process design for CO₂ capture and H₂S removal from the syngas using ionic liquid, *J Cleaner Prod* **213**: 480-490. <https://doi.org/10.1016/j.jclepro.2018.12.180>
- Yang D, Hou M, Ning H, Ma J Kang X, Zhang J and Han B (2013), Reversible Capture of SO₂ through Functionalized Ionic Liquids, *ChemSusChem* **6**(7): 1191-1195. <https://doi.org/10.1002/cssc.201300224>
- Yim J-H, Oh B-K, Lim JS (2020), Solubility Measurement and Correlation of CO₂ in bis (pentafluoroethylsulfonyl) imide ([BETI]) Anion-Based Ionic Liquids:[EMIM] [BETI], [BMIM] [BETI],[HMIM][BETI], *J Chem Eng Data* **65**(9): 4378-86. <https://doi.org/10.1021/acs.jced.0c00188>